Int J Adv Manuf Technol (2017) 91:847–858
DOI 10.1007/s00170-016-9814-7

ORIGINAL ARTICLE

Process window calculation and pressure locus optimization in hydroforming of conical box with double concave cavities

Chu Wang[1] · **Min Wan**[1] · **Bao Meng**[1] · **Long Xu**[2]

Received: 14 June 2016 / Accepted: 21 November 2016 / Published online: 29 November 2016

Abstract With the enhancement in the functional integration of components and concentration on lightweight materials, complex sheet metal parts are widely used in automobile and aviation industrial clusters. Consequently, the sheet hydroforming process has become an attractive fabricating technology for forming lightweight materials and complicated products. In this research, the hydrodynamic deep drawing (HDD) process of a composite conical box with double concave cavities was investigated through theoretical analysis, numerical simulation, and process experimentation. Furthermore, the process window diagram (PWD) was calculated using the stress analytical model combining material properties with workpiece geometrical features. The influence of cavity pressure loading locus on the forming quality of the fabricated part and the deformation behavior of aluminum alloy was explored. The forming results indicated that the initial pressure, full pressure, and loading locus are the fundamental parameters directly related to the forming quality and dimensional accuracy. For the conical part with composite features, the reasonable initial pressure value is crucial for the thickness homogeneity of the double concave characteristics, whereas the magnitude of the full pressure is vital for improving the quality of the conical feature. In addition, the optimal loading locus of the cavity pressure is characterized by two turning points, which are related to the punch corner radius, die shoulder radius, blank thickness, and angle of the conical feature.

✉ Bao Meng
mengbao@buaa.edu.cn

[1] School of Mechanical Engineering and Automation, Beihang University, Beijing, China

[2] Sheet Metal Plant, Hongdu Aviation Industry Group LTD, Nanchang, Jiangxi, China

Keywords Hydrodynamic deep drawing · Composite features · Aluminum alloy · Pressure path · Process window · Rupture and wrinkle

1 Introduction

Aluminum alloy parts formed by the deep drawing process have been significantly promoted and widely used in automotive and aviation industrial clusters in different forms, including vehicle structures, fuselage construction, and lightweight structural components, to meet the demands for structure integrity, complexity, and weight reduction of products [1–4].

In the rigid deep drawing (RDD) process, the side wall of a conical part is subjected to tensile stress along the radial direction and compressive stress along the circumferential direction during the stamping procedure [5–8]. Therefore, defects including wrinkle and rupture are the most prevalent material instabilities in the RDD process of conical part owing to the exorbitant internal compressive stress and tensile stress, respectively. These phenomena limit the types of parts and features that can be fabricated via the conventional process [9]. Especially, in the formation of conical parts, fractures and wrinkles inevitably originate on the large, unsupported region of the side wall between the punch shoulder and the die radius owing to the magnitude of compressive circumferential stress, as shown in Fig. 1. To eliminate the wrinkling phenomenon in metal formation, many attempts from theoretical analysis to experimental verification have been carried out. Wang et al. [10] derived a wrinkling criterion for sheet metal with a normal constraint using the energy method and effectively predicted the onset of the wrinkling defect. The predicted results for the formation process of a conical cup and a square cup agree well with the experimental ones. Shafaat et al. [11] carried out a new deflection function considering the effects of material anisotropy to predict the wrinkling phenomenon on the side wall

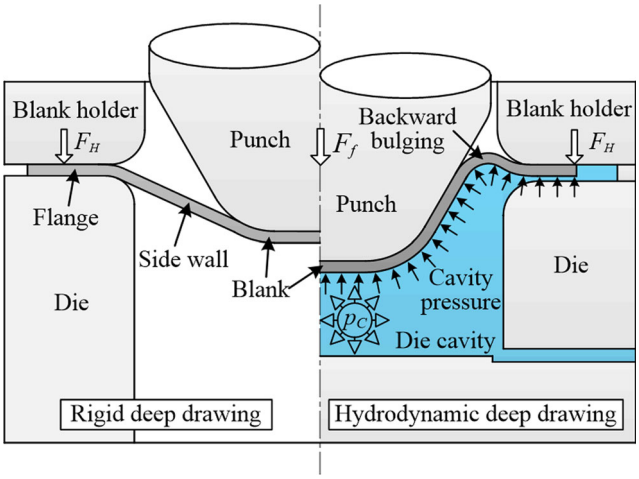

Fig. 1 Comparative schematic of the RDD and the HDD processes

area of the cup formed in the conical cup test. A good agreement between experimental data and numerical predictions using the proposed deflection function is obtained. Although the reliability of the criteria provided a robust tool in wrinkle prediction and tooling design, the origination mechanism of wrinkling on the side wall of conical parts is not systemically explored.

Compared with the RDD process, the hydrodynamic deep drawing (HDD) process takes possession of a multitude of virtues, including high dimensional accuracy, desirable surface quality, improved cold formability, less springback, and a shortened manufacturing cycle [21, 22]. During the forming period of the HDD process, a cushion of pressurized viscous fluid is generated to support the noncontact region of the workpiece. With this external support, the provided through-thickness compressive stress contributes to delay the onset of tensile instabilities and reduce the occurrence of wrinkling. Moreover, the blank is bulged backward by the pre-bulging pressure before the punch contacts the blank, which is an effective approach to avoid the origination of wrinkles on the unsupported region. Therefore, the HDD process has superior performance in terms of the avoidance of the wrinkling phenomenon because of the controllable fluid pressure. Consequently, the loading locus of cavity pressure is the vital process parameter for the success of the HDD process.

To improve the forming quality of the fabricated part, many control strategies for the cavity pressure loading locus in the HDD process have been developed. Meng et al. [12] used the HDD process to form an aluminum alloy rectangular box. The effect of cavity pressure on thickness distributions and forming defects was analyzed. The process window of cavity pressure was established based on the primary stress method, and the reasonable loading path was validated by process experiments. They found that the proper control of cavity pressure is beneficial for improving the drawability of aluminum alloys. Meng et al. [13] presented an optimized design method of drawbead parameters to change the material flow in the HDD process. The experiments were conducted with optimized parameters, and the results indicated that the method could control inner wrinkling in the HDD process effectively. Zhu et al. [14] investigated the influence of preforming depth on the multistage HDD of thin-wall cups with stepped geometries, and the sound parts were successfully formed by adopting an optimized preforming depth and pressure path. Shim and Yang [15] presented a simple method to deduce the optimal pressure curve for the sheet hydroforming process. Through a comparison between the experiment and investigation of initial and final pressures, the predicted pressure curve was verified to be an optimal one for the successful formation because no defect was observed. Abedrabbo et al. [9] analyzed the wrinkling behavior of 6111-T4 aluminum alloy during the HDD process theoretically, numerically, and experimentally. The numerical model is then used to develop an optimal pressure profile to control the wrinkle defect during the HDD process. In recent years, a few research works have been conducted to study the hydroforming of conical parts. However, an effective method to determine the pressure path in the HDD process is still a challenging problem. Yaghoobi et al. [16] built a simple theoretical model using a neural network method for the estimation of critical pressure for hydrodynamic deep drawing assisted by radial pressure (HDDRP) of conical cups. The proposed model was compared with finite element (FE) simulation and validated by experiments. They concluded that the neural network model could be applied successfully for the prediction of sheet thickness. Hashemi et al. [7] studied the process window diagram of the HDD process for the fabrication of a conical part. They found that the obtained process window diagram (PWD) could predict an appropriate forming area and probability of rupture or wrinkling occurrence under different loading loci of cavity pressure. Khandeparkar and Liewald [17] studied the ability of transferring complex features from the punch onto the blank surface through the HDD process of conical cups with complex stepped geometries. It was obtained that high pressure at the beginning of the drawing process is counterproductive.

From the foregoing brief literature review, it can be observed that the process window calculation and pressure locus optimization in hydroforming simple conical parts have been sufficiently studied. However, there are many complex conical workpieces that are characterized by conical and concave features simultaneously. During the HDD process of the multi-feature conical part, the unique method for the fast acquisition of the reasonable pressure locus and the effect of process parameters on the forming quality of the fabricated part, however, remain unknown and should be explored.

In this study, the HDD process of a composite conical part with double concave features was investigated through theoretical analysis, numerical simulation, and process experiment. The critical pressure loci for the HDD process were computed by an analytical approach combining the geometrical calculation with the stress model. In the end, the precision of the method was verified by numerical simulation and process experiment, and

the effect of the loading locus of cavity pressure on the deformation behavior of aluminum alloy and the thickness distribution of the product was also discussed.

2 Experimental procedure and numerical simulation

2.1 Part feature and material property

The shape and dimension of the conical box part are presented in Fig. 2. It is observed that there are three conical surfaces between the workpiece bottom and the flange. Owing to the particularity of the fabricated part, two types of defects are easily produced in the forming process. One is the fracture phenomenon at the juncture area between the two concave boxes owing to the severe material flow, and another is the wrinkling flaw at the conical surface due to the large unsupported area. Thus, it is crucial to control the process parameters to satisfy the requirements of the two completely reverse features, i.e., conical and concave surfaces.

The annealed aluminum alloy 2A12 with thickness of 1.0 mm was employed in the HDD process. The flow stress curve and material properties of 2A12 are presented in Fig. 3 and Table 1, respectively.

2.2 Experimental details

The HDD experiment was conducted on a special HDD equipment with the capacity of 5500 kN. The fluid pressure in the die cavity is controlled by a proportional pressure valve, and the maximum pressure can reach 100 MPa. The die sets are represented in Fig. 4.

To form the double concave features, the pre-bulging pressure is applied on the blank, and a backward bulging is produced to control the materials to flow toward the concave cavities. Subsequently, the blank is drawn into the die cavity with the movement of the punch. Meanwhile, the cavity pressure is adjusted by the relief valve to press the sheet onto the punch surface and avoid the defects of rupturing and wrinkling.

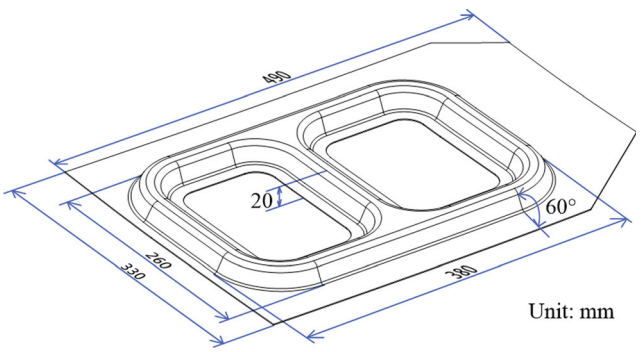

Fig. 2 The conical box with double concave features

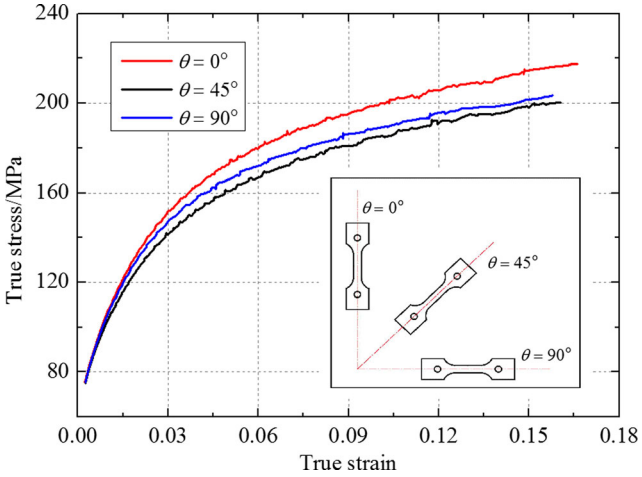

Fig. 3 The flow stress of 2A12 aluminum alloy

2.3 Numerical simulation

Numerical simulation is widely employed in the sheet metal forming process and is especially suitable for predicting the deformation process and failure modes such as wrinkling and rupture of workpieces, which can considerably reduce the time consumption and inexact and costly die tryouts.

In this research, the FE simulation is conducted on a Dynaform 5.8.1 with the LS-Dyna solver. The input models including die, blank, blank holder, and punch were constructed in the preprocessor, and the adaptive meshing is utilized for blank. The punch, the blank holder, and the die were modeled as rigid objects without elastic deformation. The blank was modeled using the four-node Belytschko-Lin-Tsay element. The three-parameter Barlat yield criterion was employed as a material model because it incorporates the effects of both normal and planar anisotropy in the yielding behavior of the material. The frictional effect was considered by using the Coulomb law. The friction coefficient between the die tooling and the blank is set to be 0.12.

Table 1 Material properties of 2A12 aluminum alloy

Parameters	Rolling direction		
	0°	45°	90°
Yielding stress, σ_s (MPa)	80.09	79.79	81.20
Ultimate tensile stress, σ_b (MPa)	174.09	173.48	186.26
Anisotropy factor, r	0.50	0.78	0.72
Strain hardening exponent, n	0.16	0.17	0.17
Young's modulus, E (GPa)	53.60	56.43	59.72
Poisson ratio, μ	0.33	0.35	0.27
Hardening coefficient, K (MPa)	276.22	276.96	295.93
Uniform elongation, δ_U (%)	15.11	16.84	16.41
Fracture elongation, δ_F (%)	15.44	17.15	16.72

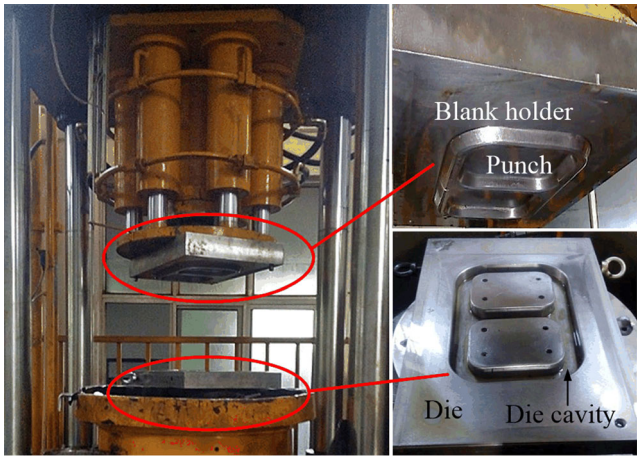

Fig. 4 The experimental setup for the HDD process

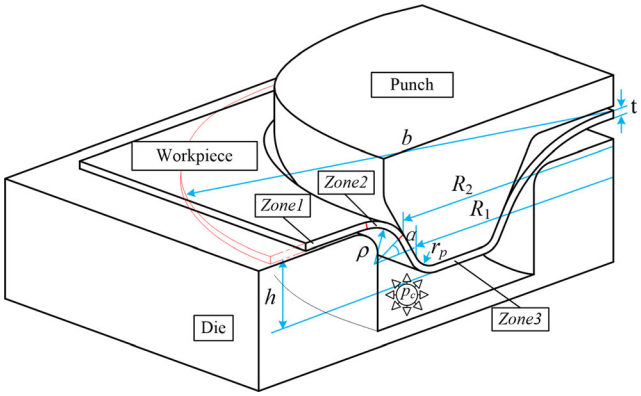

Fig. 5 Stress analysis model in the HDD process

3 Theoretical analyses of critical pressure

Considering the symmetry of the parts, one quarter of the workpiece is selected as the analysis model. Several assumptions for calculating the critical pressure are put forward as follows:

1. The volume of the workpiece is constant throughout the whole process.
2. The material follows Swift's power-hardening law, and the equivalent stress is expressed as:

$$\overline{\sigma} = K\left(\overline{\varepsilon} + \varepsilon_0\right)^n \tag{1}$$

where $\overline{\varepsilon}$, K, and n are the equivalent strain, strain hardening coefficient, and strain hardening exponent of the material, respectively.

3. The blank anisotropy can be depicted by the mean anisotropy coefficient ($\overline{R}$), as shown in Eq. (2):

$$\overline{R} = \frac{R_{0^\circ} + 2R_{45^\circ} + R_{90^\circ}}{4} \tag{2}$$

where R_{0°, R_{45°, and R_{90° are the anisotropic constants.

4. The rectangular corner blank can be transferred into one quarter of a circle with the same area as shown in Fig. 5. The equivalent radius of the rectangular corner blank is given by [23]:

$$b = \sqrt{\frac{L_{CL} \times L_{CS}}{\pi}} \tag{3}$$

where L_{CL} and L_{CS} are the length and width of the rectangular corner blank, respectively.

3.1 Stress state analysis

As depicted in Fig. 5, the workpiece in the corner area is divided into three regions according to the deformed shape including the corner flange area between the blank holder and the die (*zone 1*), the curved region in contact with the pressurized fluid (*zone 2*), and the area tightly compressed onto the surface of the punch because of the high pressure (*zone 3*) [18–20].

In this research, the HDD process of the conical box is analyzed using the Barlat-Lian yield criterion because it incorporates the effect of both normal and planar anisotropy in the yielding behavior of 2A12 aluminum alloy and is defined by the following relation:

$$f = \left|K_1 + K_2\right|^m + \left|K_1 - K_2\right|^m + \frac{u}{2-u}\left|2K_2\right|^m = \frac{u}{2-u}\overline{\sigma}^m \tag{4}$$

where K_1 and K_2 are the coefficients of the Barlat yield criterion, m is the Barlat exponent relevant to the crystal structure of the material, and u is the parameter of material anisotropy, which can be calculated according to the anisotropy factor.

In Fig. 6, for an axisymmetric radial element in the flange area, the transformation of the thickness of the corner flange is assumed to be neglected. Considering the radial and tangential directions as principal directions in this element, the

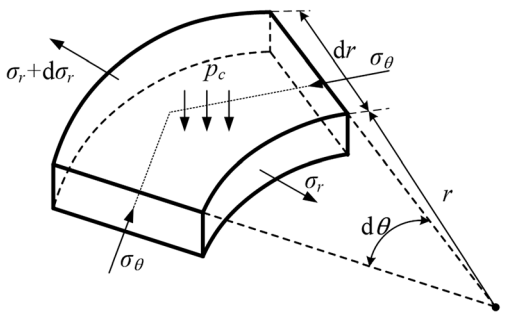

Fig. 6 Stress state of the axisymmetric element in zone 1

equilibrium equation for the flange area of the radial direction is:

$$\frac{td\sigma_{\mathrm{r}}}{dr}+\frac{t}{r}(\sigma_{\mathrm{r}}-\sigma_{\theta})+\mu p(r)=0 \tag{5}$$

where σ_{r} and σ_{θ} are the radial stress and circumferential stress, respectively. r is the radius of material point, t is the material thickness, μ is the friction coefficient between the blank and the blank holder, and $p(r)$ is the fluid pressure under the flange along the vertical direction. It is assumed that the fluid pressure linearly decreases with increasing value of r in the flange area, which can be achieved as:

$$p(r)=\frac{p_{\mathrm{c}}(b-r)}{b-d} \tag{6}$$

where p_{c} is the value of cavity pressure, and d is the sum of punch radius, die radius, and the clearance between the punch and die radii.

According to the plane strain assumption and the definition of equivalent stress, the following equation can be obtained:

$$\sigma_{\mathrm{r}}-\sigma_{\theta}=\frac{2}{\sqrt{2+c}}K\left(\frac{2}{\sqrt{2+c}}\varepsilon_{\mathrm{r}}+\varepsilon_0\right)^n \tag{7}$$

where $c=\frac{2\overline{R}}{1+\overline{R}}$.

Substituting Eq. (7) into Eq. (5) and integrating, the radial stress of the workpiece at zone 1 is:

$$\sigma_{\mathrm{r}(1)}(r)=\frac{2}{\sqrt{2+c}}K\int_r^{\mathrm{b}}\frac{1}{r}\left[\frac{2}{\sqrt{2+c}}\ln\left(\frac{r_{0(1)}}{r_{(1)}}\right)+\varepsilon_0\right]^n\mathrm{d}r+\frac{\mu p_{\mathrm{c}}(b-r)^2}{2t(b-d)} \tag{8}$$

where $r_{(1)}$ is the current radius in zone 1, and $r_{0(1)}$ is the initial radius of a supposed point in the flange region that moved to the current point with radius $r_{(1)}$.

The stress state of zone 2 is similar to that of the flange area, but there is no friction force in this region because the workpiece is completely separated from the die. The equilibrium equation in the normal direction of the workpiece as shown in Fig. 7 is:

$$\frac{\mathrm{td}\sigma_{\mathrm{r}}}{\mathrm{d}r}+\frac{t}{r}(\sigma_{\mathrm{r}}-\sigma_{\theta})=0 \tag{9}$$

With regard to the boundary condition, the radial stress in zone 2 is obtained as follows:

$$\sigma_{\mathrm{r}(2)}(r)=\frac{2}{\sqrt{2+c}}K\int_r^{R_2+t+\rho\cos\alpha}\frac{1}{r}\left[\frac{2}{\sqrt{2+c}}\ln\left(\frac{r_{0(2)}}{r_{(2)}}\right)+\varepsilon_0\right]^2\mathrm{d}r+\sigma_{\mathrm{r}(1)}(r=R_2+t+\rho\cos\alpha) \tag{10}$$

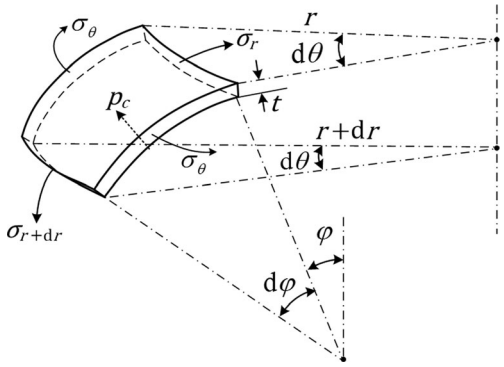

Fig. 7 Stress state of axisymmetric element in zone 2

$$R_2=R_1+\left[h-(\rho+r_{\mathrm{p}})(1-\sin\alpha)\right]\tan\alpha \tag{11}$$

where $r_{(2)}$ is the current radius in zone 2, $r_{0(2)}$ is the initial radius of the point in zone 2 that moves to the current point with radius $r_{(2)}$, and h and ρ are the height and sheet curvature of the current workpiece, respectively. In addition, R_1 is the radius of the punch in the punch shoulder area, and R_2 is the radius of the punch at the intersection point between zone 2 and zone 3.

If the cavity pressure can lift the sheet to separate from the die radius, the stress in zone 3 is:

$$\sigma_{\mathrm{r}(3)}(r)=-\frac{\mu p_{\mathrm{c}}(r-\rho)}{t\cdot\cos\alpha}+\sigma_{\mathrm{r}(2)}(R_2) \tag{12}$$

It is observed that there is hardly any friction between the punch and the blank in zone 3 when the cavity pressure is quite low, and the radial tensile stress reaches the maximum value at the punch shoulder region. Conversely, when the cavity pressure is high enough, the beneficial friction is generated between the punch and the blank because the oil is pressed out under the blank flange, and the dangerous section will transfer to the area around the die radius, i.e., zone 2.

3.2 Critical rupture cavity pressure

The maximum tensile stress of the unsupported area should not exceed the tensile strength of the used material, which is the principle to calculate the upper limit of the cavity pressure loading locus. The balance equation in the forming process and the force (F) exerted on the sheet are calculated by:

$$\frac{\pi}{4}p_{\mathrm{c}}\left[(R_2+\rho\cdot\cos\alpha)^2-(R_2+t\cdot\cos\alpha)^2\right]=\frac{2}{4}\pi R_2 t\sigma_{\mathrm{r}(2)}(R_2) \tag{13}$$

$$F=\frac{\pi}{2}tR_2\sigma_{\mathrm{r}}+\frac{\pi}{4}\mu p_{\mathrm{c}}\cdot(R_1+R_2)\cdot\left[(\rho+r_{\mathrm{p}})(1-\sin\alpha)\right] \tag{14}$$

where $\sigma_{\mathrm{r}}=\frac{2}{\sqrt{4-c^2}}\overline{\sigma}$. The necking condition occurs around the punch corner, and the forming force curve experiences the

maximum point (dF = 0). Taking the derivative of Eq. (14), the following equation can be obtained:

$$\frac{d\overline{\sigma}}{d\overline{\varepsilon}} = \frac{\sqrt{4-c^2}}{2}\overline{\sigma} \tag{15}$$

According to Swift's power-hardening law, the critical effective strain is obtained by:

$$\overline{\varepsilon}_{\mathrm{cr}} = \frac{2n}{\sqrt{4-c^2}} - \overline{\varepsilon}_0 \tag{16}$$

With the plane strain condition, substituting Eq. (16) and $h = (\rho + r_{\mathrm{p}})(1 - \sin\alpha)$ into Eq. (13), the critical stress is obtained as follows:

$$\sigma_{\mathrm{cr}} = \frac{2F_{\mathrm{c}}}{\pi t R_2} = K\left(\frac{2n}{\sqrt{4-c^2}}\right)^n \tag{17}$$

When the cavity pressure is exceedingly higher, the fracture generally appears around the die radius area. Therefore, the critical rupture occurs with:

$$\sigma_{\mathrm{cr}} = \sigma_{\mathrm{r}(2)}(R_2) \tag{18}$$

The blank is separated from the die corner under the effect of cavity pressure to reduce the friction between the blank and the die. The fluid pressure in the flange area is zero when the workpiece is exactly separated from the die radius. According to the geometric critical condition ($\rho = r_{\mathrm{d}}$) and equilibrium equation, i.e., Eq. (13), the lower critical cavity pressure can be presented as Eq. (19):

$$p_{\mathrm{l}} = \left.\frac{2tR_2 \cdot \sigma_{\mathrm{r}(2)}(R_2)}{(r_{\mathrm{d}} - t)\cdot\cos\alpha[2R_2 + (r_{\mathrm{d}} + t)\cdot\cos\alpha]}\right|_{p(r)=0} \tag{19}$$

In Eq. (19), r_{d} is the die radius. The flowchart of the calculation procedure for the critical loading loci is represented in Fig. 8. All calculations were processed utilizing Newton's method in the MATLAB numerical computing language. The initial values of h_0 and ρ_0 are set as 0 and r_{d}, respectively. Furthermore, the values of Δh and $\Delta\rho$ are specified to be 0.05 and 0.1 mm, respectively.

4 Results and discussion

The lower critical pressure and the upper critical pressure can be calculated via the analytical model together with the material properties and the geometrical dimensions of the final shape. Figure 9a depicts the PWD in the formation of the conical part using the HDD process based on the analytical model. The relationship between the reasonable cavity pressure and the punch stroke during the HDD process is a significant challenge. On the one hand, the material will bend to the radius of curvature of the punch much faster than the allowed ductility of the material when the pressure is higher than the upper critical pressure curve, which will lead to the rupture of the workpiece around the die shoulder. On the other hand, the material flow resistance is increased and the sheet is unable to be entirely separated from the die radius if the cavity pressure is smaller than the lower critical pressure. In turn, the sharp thinning around the punch radius is grown, which also results in the rupture of the part. Consequently, the safe area between the upper and lower critical profiles can provide reasonable cavity pressure versus punch stroke locus to ensure a flawless part. The objective part takes possession of conical and concave features. It is much more difficult to optimize the loading locus of cavity pressure to meet the requirements of these two features.

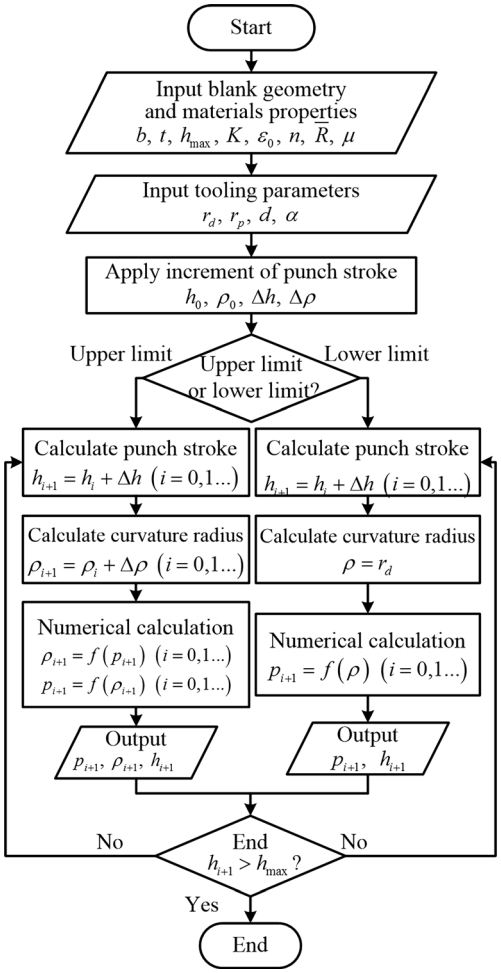

Fig. 8 The calculation procedure for the critical loading loci of the cavity pressure

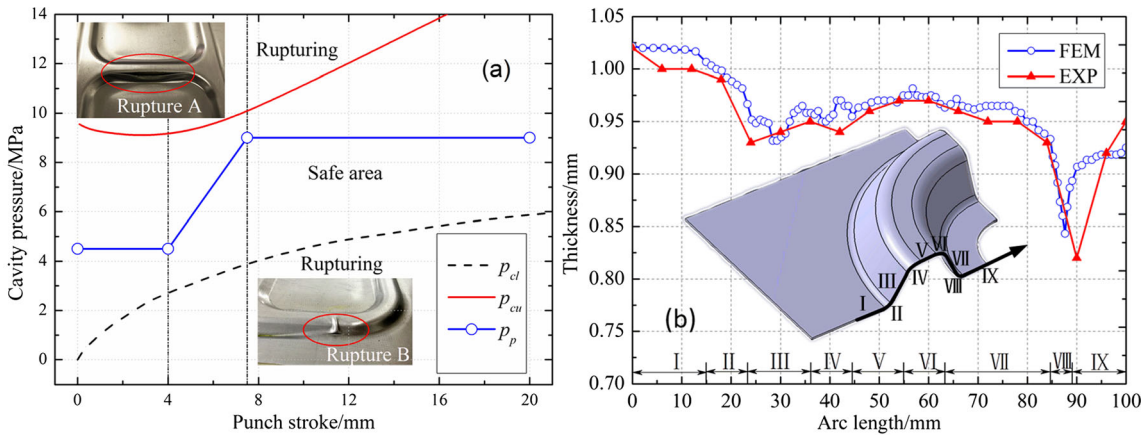

Fig. 9 The validation of FE simulation: **a** PWD of the HDD process and **b** wall thickness distribution of FE simulation and experiment

4.1 Validation of FE model

A new type of cavity pressure loading locus was put forward as shown in Fig. 9a with initial cavity pressure p_i = 4.5 MPa and maximum cavity pressure p_{max} = 9 MPa. Furthermore, the corresponding numerical simulation and experimental test were carried out. As shown in Fig. 9a, two types of tearing defects easily appear during the HDD process. One occurs around the punch corner due to the insufficient of initial cavity pressure, while another turns up around the die entrance owing to the excessive cavity pressure. To verify the accuracy of the FE model, a comparative study on the wall thickness distribution of the workpiece formed with the proposed loading locus between the numerical results and experimental ones was conducted, as depicted in Fig. 9b. In the figure, the wall thickness distribution of the fabricated part was measured along the direction containing both conical and concave features. It is found that the two results are in excellent agreement. Meanwhile, the results of the experiment and numerical simulation demonstrate the effectiveness of the process analysis and PWD in the HDD process.

4.2 Parametric analysis

The HDD process is mainly determined by the loading locus of cavity pressure, which is characterized by the initial pressure, the maximum pressure, and the pressure profile. Insufficient initial pressure cannot cleave the blank from the die orifice, and the rupture defect easily appears at the punch shoulder. However, an exceedingly high initial pressure leads to the bulge formation and fracture defect on the unsupported blank between the punch and the blank holder, whereas insufficient cavity pressure leads to rupture defect around the punch shoulder. However, excessive cavity pressure may cause the leakage of fluid between the die and the blank, which prevents the materials from flowing into the die cavity and results in severe thinning of wall thickness around the die entrance area.

4.2.1 Effect of initial cavity pressure

The blank cannot be lifted up from die surface as the punch penetrates into the die cavity with a low initial pressure and thus causes the process instability. The minimum required

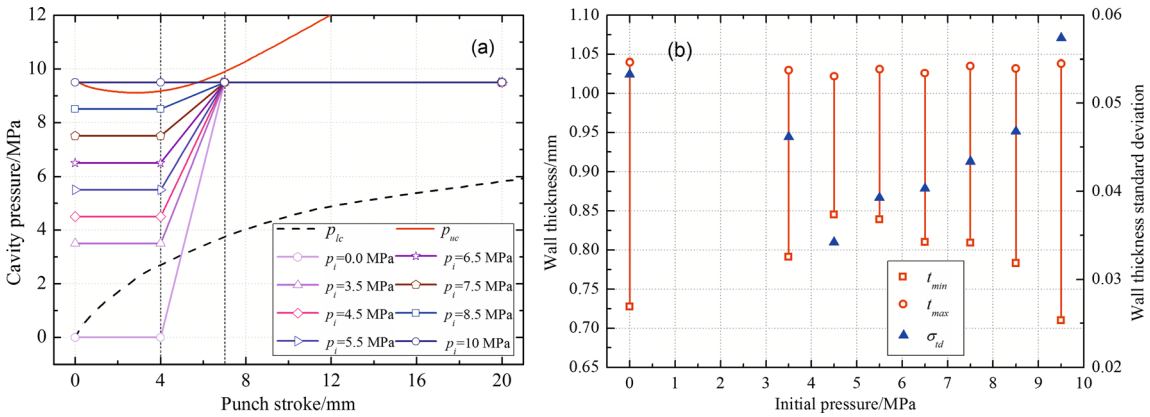

Fig. 10 Effect of p_i on the wall thickness: **a** loading loci with different p_i and **b** t_{max}, t_{min}, and σ_{td} distributions

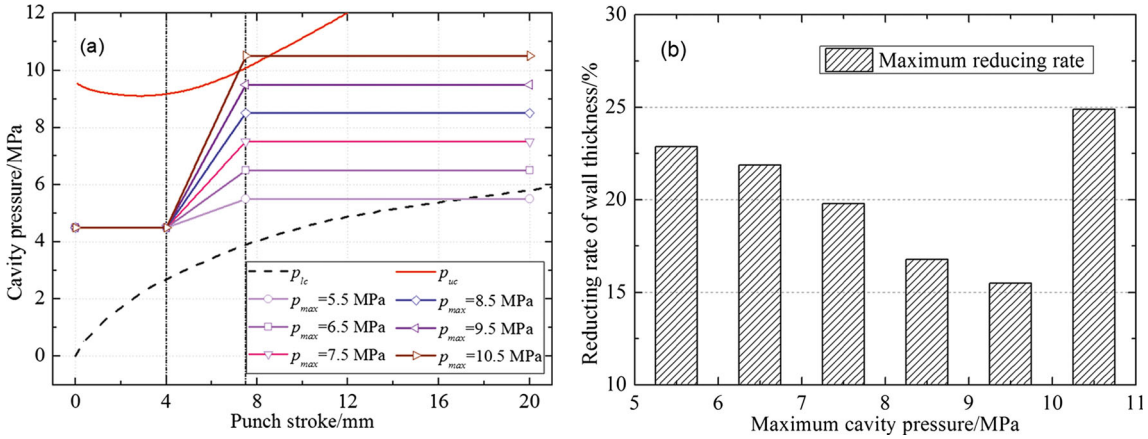

Fig. 11 Effect of p_{max} on wall thickness: **a** loading loci with different p_{max} and **b** maximum reducing rate of wall thickness

initial pressure becomes $p_i \geq \frac{4d_{eq}t\sigma_s}{\sqrt{3}\left(D_{eq}^2-d_{eq}^2\right)}$, where d_{eq} is the equivalent diameter of the blank, D_{eq} is the equivalent diameter of blank contact region to the punch at initial stage, σ_s is the tensile yield stress, and β is the correction factor to compensate forming difficulty due to shape of cross section [15].

To investigate the influence of initial pressure (p_i) on the HDD process, several cavity pressure loading loci with diverse initial pressures were proposed, as shown in Fig. 10a. The simulation results of the maximum wall thickness (t_{max}), the minimum wall thickness (t_{min}), and the standard deviation of wall thickness (σ_{td}) are illustrated in Fig. 10b. σ_{td} is defined as $\sigma_{td} = \sqrt{\sum_{i=1}^{N}(t_i-\bar{t})^2/N}$, where N is the number of nodes in the simulation results, t_i is the

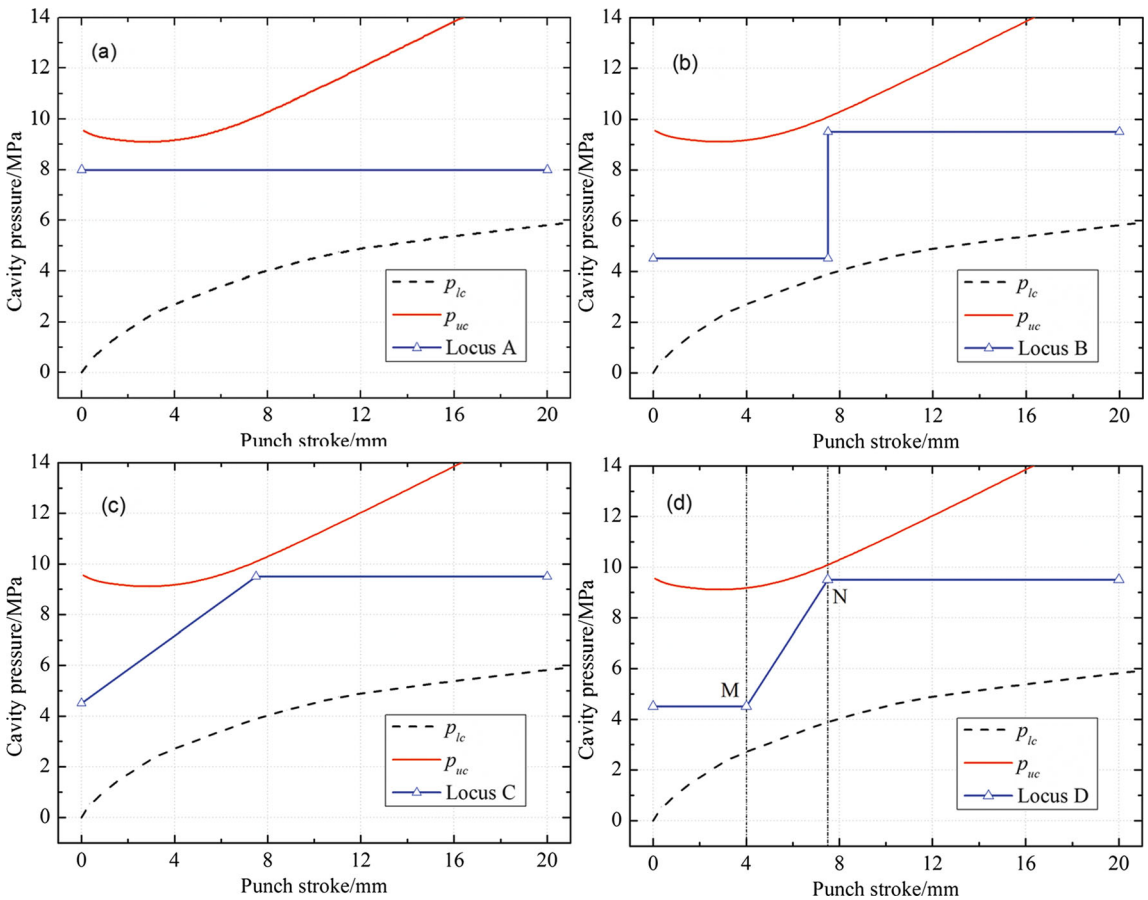

Fig. 12 Cavity pressure loading loci with different profiles: **a** locus A, **b** locus B, **c** locus C, and **d** locus D

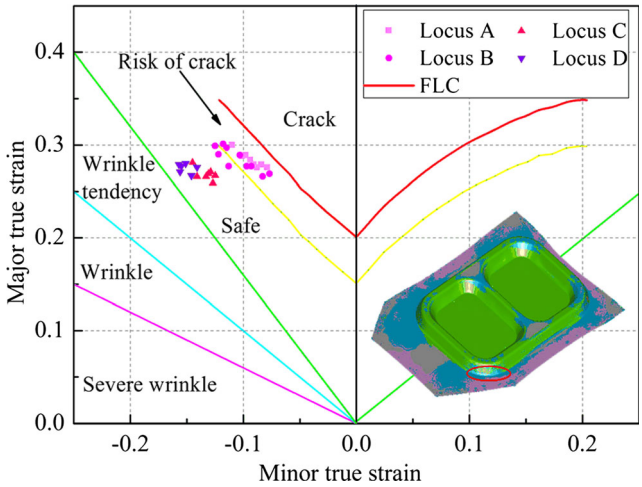

Fig. 13 FLC with different profiles of loading loci

thickness of node, and $\bar{t}$ is the mean value of the thickness. It is indicated that the values of t_{max} at various initial pressures are similar. Meanwhile, t_{min} increases with increasing p_i until it reaches a peak value of 4.5 MPa and follows a downward trend between 4.5 and 9.5 MPa. Because of the inapposite initial cavity pressure, the thickness decreased by 28 and 29.5 % when the initial cavity pressures are 0 and 7.5 MPa, respectively. It can be observed in Fig. 10b that a severe thinning phenomenon appears around the punch corner or the die entrance when the initial cavity pressure is too low or two high, which agrees well with the calculated PWD.

The wall thickness evenness is intuitively reflected by σ_{td} because of the standard deviation; this is an index that is used to quantify the amount of data values. The trend in the change of σ_{td} is opposite to that of t_{min}, and σ_{td} reaches the valley value at 4.5 MPa. It is concluded that excessively high or low pressure is not conducive to the uniformity of wall thickness. Therefore, a reasonable initial pressure obtained by the numerical result is approximately 4.5 MPa.

In the preliminary stage of the HDD process, the blank is not fully covered by the punch. If the initial pressure is too low, the friction retention and fluid lubrication effect cannot act in the HDD process, and the thickness will become significantly thinner. However, excessive initial pressure may lead to severe thinning of the workpiece because the blank will be bulged into the punch with a large size under high cavity pressure.

4.2.2 Effect of maximum cavity pressure

With the determined initial pressure and the assumption of pressure path for which the pressure is proportional to the punch penetration travel, numerical simulations were carried out for some trial final pressure values. Several cavity pressure loading loci with the same initial pressure (4.5 MPa) and the different maximum pressures varying from 5.5 to 10.5 MPa were proposed to investigate the effect of the maximum cavity pressure on the HDD formability, as shown in Fig. 11a. Meanwhile, the maximum reducing ratios of wall thickness of each loading locus are illustrated in Fig. 11b.

As the maximum cavity pressure increases from 5.5 to 9.5 MPa, the maximum reducing ratio of the wall thickness decreases from 22.8 to 15.4 %. Therefore, the reducing ratio of the workpiece wall thickness is reduced by increasing the maximum cavity pressure within a proper range from 5.5 to 9.5 MPa. This is because high pressure can promote the occurrence of beneficial friction between the workpiece material and the punch nose. Meanwhile, the radial tensile stress in the workpiece is restrained, and the deducting ratio is reduced. Owing to the occurrence of adverse friction, excessive pressure may cause a higher reduction of thickness or even lead to ruptures turning up around the die entrance. Consequently, the optimal value of the maximum cavity pressure is 9.5 MPa for the conical part.

4.2.3 Effect of locus profile

To investigate the effect of the locus profile on the forming quality of the fabricated part in the HDD process, several cavity pressure loading loci with the same maximum pressure (except

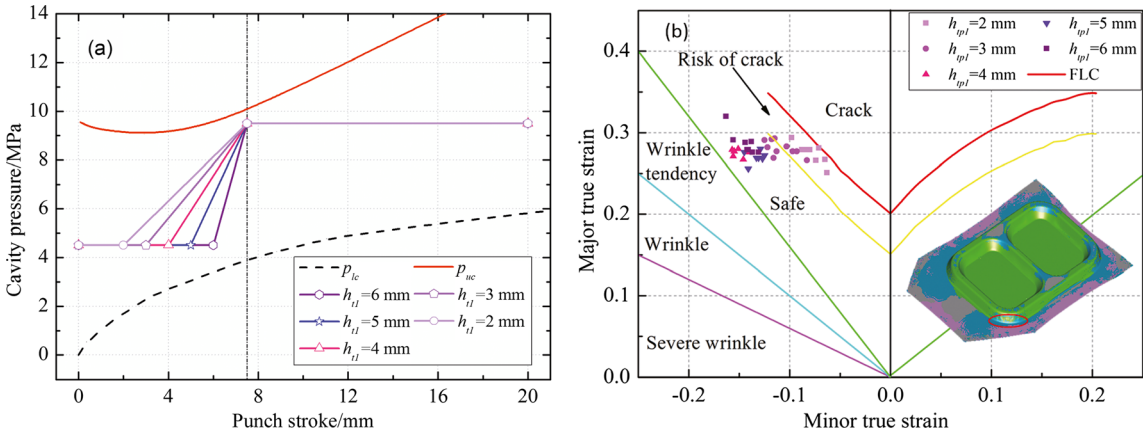

Fig. 14 Effect of p_{tp1} on wall thickness: **a** loading loci with different h_{tp1} and **b** FLD with different h_{tp1}

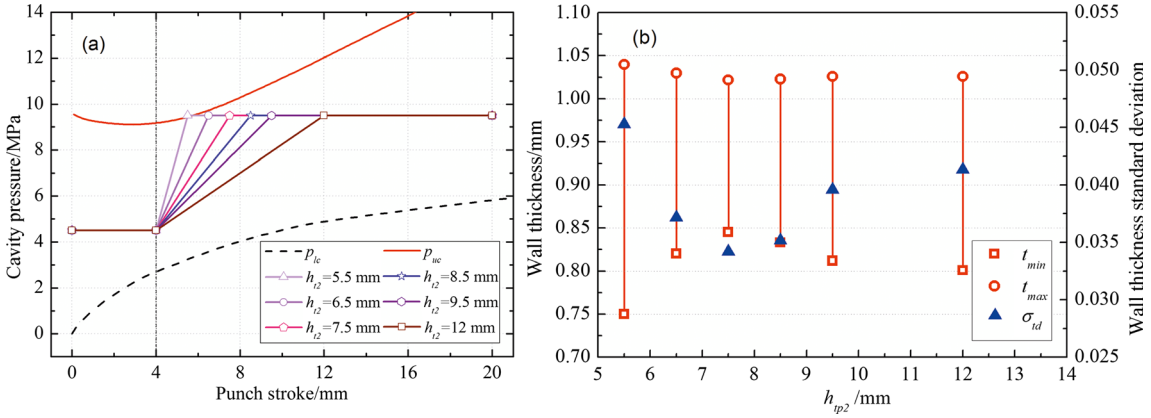

Fig. 15 Effect of h_{tp2} on wall thickness: **a** loading loci with different h_{tp2} and **b** t_{max}, t_{min}, and σ_{td} distributions

locus A) and different locus profiles were proposed, as shown in Fig. 12. To evaluate the different locus profiles of cavity pressure, the forming limit curve (FLC) is used. Owing to the forming defects that easily appear around the selected area in Fig. 13, the major and minor true strains in the corresponding areas of different profiles are mapped in Fig. 13.

It is obtained that some measuring points of loci A and B are very close to the FLC. Although there is no obvious fracture defect in the numerical simulation result, serious necking was observed in the unsupported area between the punch and the die. This indicates that the excessive or insufficient initial pressures increase the risks of rupture in the unsupported region and punch corner. Locus C is a typical loading locus of cavity pressure for the HDD process of the axisymmetric cup-shape part [6, 16]. However, it is observed that measuring points of locus C are slightly closer to the necking line compared with those using locus D. This phenomenon is mainly because the pre-bulging process has a significant impact on the forming quality of the fabricated part. For the proposed loading locus D, the double concave features are preformed to contact the punch with the effect of cavity pressure before the punch reaches the sheet. Thus, the beneficial friction between the punch and the blank increases, and the trend of fracture around the punch corner decreases because of the pre-bulging effect. In this case, a part of the concave feature of the workpiece is generated before the punch moves, and the inward flow of the material is also beneficial to further deformation.

It is observed that there are two turning points M and N in loading locus D as shown in Fig. 12d. To investigate the effect of turning points on the material formability in the HDD process, several loading loci of cavity pressures with different turning points are proposed as depicted in Figs. 14 and 15. The punch strokes corresponding to the first turning point M and the second turning point N are denoted as h_{tp1} and h_{tp2}, respectively. As represented in Fig. 14b, the simulative results show that t_{min} increases with increasing h_{tp1} from 2 to 4 mm and decreases when h_{tp1} exceeds 4 mm. It is observed that the optimal value of h_{tp1} is 4 mm, which satisfies the following equation:

$$h_{tp1} = r_p \cdot (1 - \cos\alpha) + t \tag{20}$$

When $h_{tp1} < [r_p \cdot (1 - \cos\alpha) + t]$, the punch corner has not been fully formed before the increase in the cavity pressure, which leads to the local thinning around the punch corner. Conversely, if $h_{tp1} > [r_p \cdot (1 - \cos\alpha) + t]$, the friction increases, and the fluid lubrication effect cannot act on the workpiece.

Regarding the second turning point N, the optimal value satisfies the following equation:

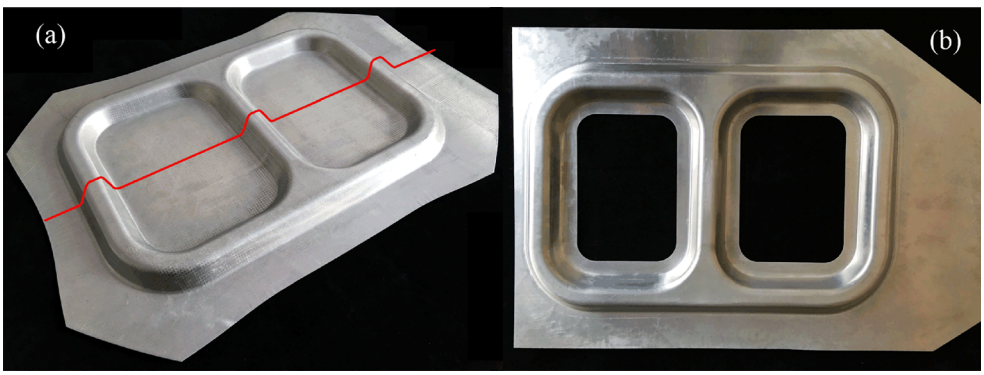

Fig. 16 **a**, **b** Parts formed by the HDD process with optimal loading locus

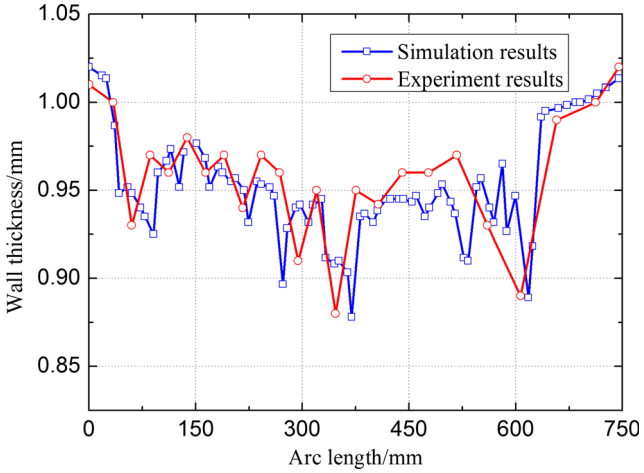

Fig. 17 The thickness distributions of the experimental part and the numerical result

$$h_{tp2} = r_d + r_p \cdot (1 - \cos\alpha) + t \tag{21}$$

As shown in Fig. 15b, when $h_{tp2} < [r_d + r_p \cdot (1 - \cos\alpha) + t]$, the conical wall of the workpiece has not been formed. Therefore, there is no beneficial friction between the punch and the blank to support the materials drawing into the die, which results in excessive thinning of the materials in the unsupported area. Conversely, if $h_{tp2} > [r_d + r_p \cdot (1 - \cos\alpha) + t]$, the blank cannot be separated from the die corner with the effect of cavity pressure in the early stage of deformation of the conical wall, which results in severe thinning of the materials in the die corner area.

Based on the proposed numerical simulation, the optimal loading locus of cavity pressure characterized by an initial pressure of 4.5 MPa, a maximum pressure of 9.5 MPa, and two optimal turning points was obtained. After obtaining the optimized pressure profile, the validity of the process parameters is tested by the HDD process experiment. The formed part without wrinkling and rupture is depicted in Fig. 16b, which was partitioned along the diagonal line illustrated in Fig. 16a. The thickness distributions of the experimental part and the numerical result are shown in Fig. 17, and it is observed that the results of the process experiment agree well with the simulative ones.

5 Conclusions

In this research, the effect of the loading locus on aluminum alloy deformation was investigated utilizing the HDD process of a conical box with double concave features. The critical pressure and PWD were proposed via a stress analytical model. Furthermore, the accuracy of the PWD was verified by the numerical simulation and experimental process. The effect of the die cavity pressure loading locus on the forming quality of the product was explored, and the measures to promote the sheet formability were also discussed. The conclusions have been drawn as follows:

1. The theoretical analysis approach of the aluminum alloy complex conical part in the HDD process is established by the combination of geometrical calculation and the stress model. The lower and upper critical pressures are closely related to material properties and part geometrical features.
2. A reasonable initial pressure is crucial for the thickness homogeneity of the double concave features of the conical part. The minimum wall thickness and the evenness of the wall thickness increase with increasing initial pressure within the range from 2.5 to 4.5 MPa. Excessive or insufficient initial pressure is not conducive to the reduction of wall thickness thinning and the uniformity of wall thickness.
3. The value of the maximum pressure is vital for improving the quality of the conical feature. The reduction ratio of the workpiece wall thickness is reduced, and the thickness evenness improved by increasing the maximum cavity pressure within a proper range from 5.5 to 9.5 MPa.
4. The optimized loading locus of cavity pressure is mainly determined by two turning points. The optimal values of the two turning points are $[r_p \cdot (1 - \cos\alpha) + t]$ and $[r_d + r_p \cdot (1 - \cos\alpha) + t]$, respectively.

Acknowledgements This project is supported by the National Natural Science Foundation of China (Grant Nos. 51605018 and 51275026).

References

1. Zhang SH, Wang ZR, Xu Y, Wang ZT, Zhou LX (2004) Recent developments in sheet hydroforming technology. J Mater Proc Tech 151:237–241
2. Lang L, Danckert J, Nielsen KB (2004) Study on hydromechanical deep drawing with uniform pressure onto the blank. Int J Mach Tool Manu 44:495–502
3. Dursun T, Soutis C (2014) Recent developments in advanced aircraft aluminium alloys. Mater Des 56:862–871
4. Singh SK, Ravi Kumar D (2008) Effect of process parameters on product surface finish and thickness variation in hydro-mechanical deep drawing. J Mater Proc Tech 204:169–178
5. Chen Y, Liu W, Xu Y, Yuan S (2015) Analysis and experiment on wrinkling suppression for hydroforming of curved surface shell. Int J Mech Sci 104:112–125
6. Wang H, Gao L, Chen M (2011) Hydrodynamic deep drawing process assisted by radial pressure with inward flowing liquid. Int J Mech Sci 53:793–799
7. Hashemi A, Hoseinpour GM, Seyedkashi SMH (2015) Process window diagram of conical cups in hydrodynamic deep drawing assisted by radial pressure. T Nonferr Metal Soc 25:3064–3071
8. Bagherzadeh S, Mirnia MJ, Mollaei Dariani B (2015) Numerical and experimental investigations of hydro-mechanical deep drawing process of laminated aluminum/steel sheets. J Manu Proc 18:131–140
9. Abedrabbo N, Zampaloni MA, Pourboghrat F (2005) Wrinkling control in aluminum sheet hydroforming. Int J Mech Sci 47:333–358

10. Wang X, Cao J (2000) On the prediction of side-wall wrinkling in sheet metal forming processes. Int J Mech Sci 42: 2369–2394
11. Shafaat MA, Abbasi M, Ketabchi M (2011) Investigation into wall wrinkling in deep drawing process of conical cups. J Mater Proc Tech 211:1783–1795
12. Meng B, Wan M, Yuan S, Xu X, Liu J, Huang Z (2013) Influence of cavity pressure on hydrodynamic deep drawing of aluminum alloy rectangular box with wide flange. Int J Mech Sci 77:217–226
13. Meng B, Wan M, Wu X, Yuan S, Xu X, Liu J (2014) Inner wrinkling control in hydrodynamic deep drawing of an irregular surface part using drawbeads. Chinese J Aeronaut 27:697–707
14. Zhu Y, Wan M, Zhou YK (2012) Investigation into influence of preforming depth on multi-stage hydrodynamic deep drawing of thin-wall cups with stepped geometries. Adv Mater Res 457-458:1219–1222
15. Shim H, Yang DY (2005) A simple method to determine pressure curve for sheet hydro-forming and experimental verification. J Mater Proc Tech 169:134–142
16. Yaghoobi A, Baseri H, Bakhshi-Jooybari M, Gorji A (2013) Pressure path optimization of hydrodynamic deep drawing of cylindrical-conical parts. Int J Precis Eng Man 14:2095–2100
17. Khandeparkar T, Liewald M (2008) Hydromechanical deep drawing of cups with stepped geometries. J Mater Proc Tech 202:246–254
18. Jalil A, Hoseinpour GM, Sheikhi MM, Seyedkashi SMH (2016) Hydrodynamic deep drawing of double layered conical cups. T Nonferr Metal Soc 26:237–247
19. Bagherzadeh S, Mollaei-Dariani B, Malekzadeh K (2012) Theoretical study on hydro-mechanical deep drawing process of bimetallic sheets and experimental observations. J Mater Proc Tech 212:1840–1849
20. Assempour A, Taghipour E (2011) The effect of normal stress on hydro-mechanical deep drawing process. Int J Mech Sci 53:407–416
21. Zhang SH (1999) Developments in hydroforming. J Mater Proc Tech 91:236–244
22. Zampaloni M, Abedrabbo N, Pourboghrat F (2003) Experimental and numerical study of stamp hydroforming of sheet metals. Int J Mech Sci 45:1815–1848
23. E DX, Mizuno T, Li Z (2008) Stress analysis of rectangular cup drawing. J Mater Proc Tech 205:469–476